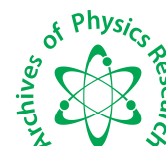




Scholars Research Library

Archives of Physics Research, 2012, 3 (5):401-406
(<http://scholarsresearchlibrary.com/archive.html>)



Scholars Research
Library

ISSN : 0976-0970

CODEN (USA): APRRC7

Role of concentration and temperature on well-aligned ZnO nanorod by low-temperature wet chemical bath deposition method

G. R. Patil,^a R.S. Gaikwad,^a M.B.Shelar,^b R. S. Mane,^c S.H. Han^d and B. N. Pawar,^{a*}

^a Department of Physics, Bharati Vidyapeeth University, Pune-411038, Maharashtra, India

^b Department of Physics, Shivaji University, Kolhapur, Maharashtra, India

^c Centre for Nanomaterials and Energy Devices, School of Physical Sciences, Swami Ramand Teerth Marathwada University, Nanded, India.

^d Nanomaterials Laboratory, Department of Chemistry, Hanyang University, Seoul 133-791, Seoul, Republic of Korea.

ABSTRACT

Well-aligned ZnO nanorod arrays were synthesized by low-temperature wet chemical bath deposition (CBD) method on Si substrate under different conditions. Results illustrated that dense ZnO nanorods with hexagonal wurtzite structure were vertically well-aligned and uniformly distributed on the substrate. The effects of precursor concentration and growth temperature on nanorods morphology were investigated systematically. The mechanism for the effect of preparation parameters was elucidated based on the chemical process of CBD and basic nucleation theory. It is demonstrated that the controllable growth of well-aligned ZnO nanorods can be realized by readily adjusting the preparation parameters. Strong near-band edge ultraviolet (UV) emission were observed in room temperature absorbance spectra for the samples prepared under optimized parameters, yet the usually observed defect related deep level emissions were nearly undetectable, indicating high optical quality ZnO nanorod arrays could be achieved via this easy process chemical approach at low temperature.

Keywords: ZnO, CBD, nanorods, UV absorbance.

INTRODUCTION

One-dimensional (1D) nanostructure materials have been extensively studied because of their potential applications in nanoelectronic devices, such as field-effect transistors [1], single electron transistors [2], photodiodes [3], and chemical sensors [4]. Among these 1D semiconducting nonmaterial's, there has been considerable attention focused on low-dimensional ZnO nanostructures on account of its many exciting properties, such as a wide band gap (3.37 eV), a large exciton binding energy (60 meV), excellent chemical and thermal stability, transparency, biocompatibility, and wide electrical conductivity range [5]. ZnO has probably the richest family of nanostructures among all materials, which exhibits the most splendid and abundant configurations of nanostructures that one material can form. An up-to-date comprehensive review on ZnO nanomaterial platform for nanotechnology can be found in Ref. [6]. Single crystal ZnO nanorod is of particular interest due to its potential applications in an emerging area of nanotechnology. Up to now, numerous experimental attempts have been reported to fabricate ZnO nanorod materials, such as molecular beam epitaxy (MBE) [7], pulsed laser deposition (PLD) [8], sputtering [9], electrochemical deposition [10], vapor phase transport (VPT) [11], chemical vapor deposition (CVD) [12], thermal

evaporation [13]. However, these methods usually require expensive equipment's and high operation temperature, which are not compatible with organic substrates for applications in flexible and wearable electronics. Compared with the methods mentioned above, the wet chemical bath deposition (CBD) method as a high performance growth technique for ZnO nanorod/nanowire is especially attractive due to its obvious advantages of low-cost, low-temperature operation and environmental friendliness. Moreover, this technique can be carried out at low temperatures and large scale on any substrate, regardless of whether it is crystalline or amorphous [14, 15]. An important and key issue for the technological applications of ZnO nanorods is to realize the controllable growth for desired functionality and put it into practice. Therefore, fundamental understanding of the effects of preparation parameters and growth mechanism are essential. In this paper, the wet CBD method was employed to fabricate ZnO nanorods on Si substrate and the special attention was paid to the effect of the precursor concentration, growth temperature and time on the morphology of as-grown ZnO nanorods. It should be noted that only strong near-band edge UV emission peak were observed in room temperature absorbance spectra for the samples under optimized parameters, indicating high optical quality ZnO nanorod arrays could be achieved via this low-temperature easy process chemical approach. The achievement of well-aligned ZnO nanorod arrays with high optical quality and uniform thickness and length distributions is of considerable interest because they are highly appropriate for further fabrications of vertical nano device arrays.

MATERIALS AND METHODS

2 Experimental Details

CBD technique has been proven to be a good approach for synthesis of ZnO nanorods with the use of ZnO seeds in the forms of thin films [16]. Here, Si was chosen as a substrate for ZnO nanorod arrays grown using a CBD technique. The Si substrates were cleaned in the ultrasonic bath with acetone, ethanol and deionized water to remove adsorbed dust and surface contamination. In order to fabricate vertically aligned nanorods, ZnO seed layer was first fabricated on the substrates by simple silar method. 100ml aqueous solutions composed of zinc acetate ($\text{Zn}(\text{CH}_3\text{COO})_2 \cdot 2\text{H}_2\text{O}$) with ammonia solution were used as a precursor source for the growth of ZnO nanorods. All the employed chemicals were analytical reagent grade. The concentration of $\text{Zn}(\text{CH}_3\text{COO})_2 \cdot 2\text{H}_2\text{O}$ was varied in the range of 0.025 to 0.075M while keeping the molar ratio of $\text{Zn}(\text{CH}_3\text{COO})_2 \cdot 2\text{H}_2\text{O}$ and ammonia to be 1:1. The solution was then transferred into a sealable glass beaker in which the substrates were suspended vertically. The optimized films with precursor concentration were taken for growth temperature variation in the range of 65°C to 95°C. At the end of the growth, the substrates were taken out of the solution and rinsed several times with deionized water, and then blew dried with high purity Ar gas at room temperature. A detailed chemistry process by CBD technique can be found elsewhere [17].

A Philips Japan MPD 1880 X-ray powder diffractometer was employed to study the crystal structure of the films. Surface morphology of the films was examined by scanning electron microscopy, SEM (JEOL, 15 kV). A Shimadzu double beam spectrophotometer was employed for obtaining absorbance in the wavelength range of 350–800 nm and to evaluate the direct band gap energies.

RESULTS AND DISCUSSION

Fig. 1 shows the typical XRD pattern for the as-grown ZnO nanorod arrays grown on Si substrate. All diffraction peaks are consistent with the wurtzite structure, which can be indexed to a standard spectrum of JCPDS (No. 36-1451). For all the samples, the (0 0 2) diffraction peak in XRD patterns is dominant, which reveals the preferentially oriented growth along the c-axis.

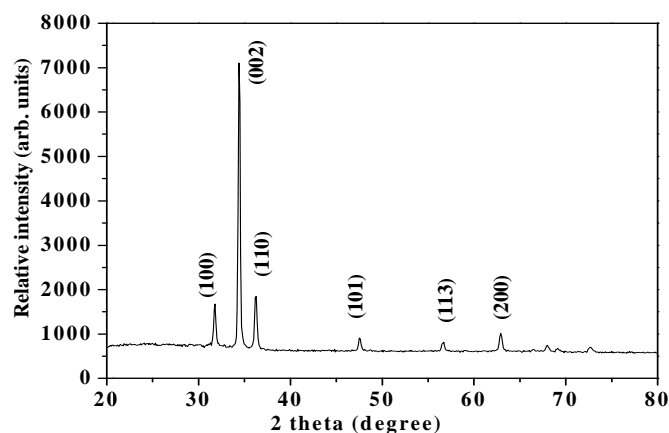


Fig1: XRD pattern of as grown ZnO nanorod arrays.

A series of experiments were performed by varying the precursor concentration but keeping other parameters constant to investigate the effect of the precursor concentration on the morphology and aspect ratio of ZnO nanorod arrays. Fig. 2 shows the SEM images of ZnO nanorod arrays grown with the precursor concentration varied from 0.025M to 0.075M. The growth temperature and time were 85°C and 2h, respectively. It can be clearly seen that the morphology of as-grown ZnO nanorod arrays are closely related to the precursor concentration. Furthermore, it shows that initially for low precursor concentration each nanorod has change in diameter along its entire length, and are small in size indicating that the growth anisotropy is constantly changing but for 0.075M concentration growth anisotropy is constantly maintained and well grown nanorods are formed. Fig. 2 shows that the ZnO nanorod arrays possessed an average variation in nanorod diameter with increase in precursor concentration but poor preferred orientation. The ZnO samples prepared from 0.025M and 0.05M zinc acetate solution possess highly oriented nanorod arrays with high density, which is due to the fact that the nucleation density on the Si substrate increases as the Zn concentration in the solute on increases. As the solution concentration increases above 0.05M, it is very obvious that the average diameter is dramatically increased by the clustering of nanorods, which leads to lower aspect ratio and may also worsen the degree of nanorod orientation. However, for samples under higher precursor concentration, are dense ZnO nanorod arrays with a hexagonal wurtzite structure were vertically well-aligned and uniformly distributed on the Si substrate.

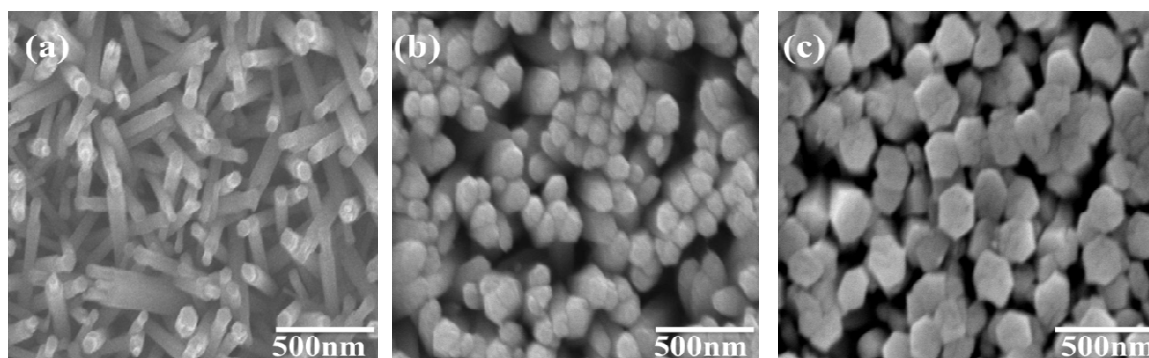


Fig 2: SEM micrograph of precursor dependent ZnO thin films (a) 0.025M (b) 0.05M (c) 0.075M.

To study the effect of growth temperature on the morphology of ZnO nanorod arrays, CBD growth of the ZnO nanorod arrays were performed on Si substrate from 65 °C to 95 °C with the optimized precursor concentration of 0.075M for 2 h. The corresponding SEM images of the nanorods grown at each temperature are shown in Fig. 3. It shows that nearly all the ZnO nanorods are perpendicularly oriented to the substrate regardless of the growth temperature. Top-view SEM images reveal that the nanorods are hexagonal prism shape, suggesting that the nanorods grow along [0 0 2] direction at various temperatures. However, the growth temperature has a strong impact

on the diameter and length of the nanorods. As shown in Fig. 3a–d, the average diameter, length and aspect ratio increased dramatically with the increase of growth temperature upto 85°C and further decreased with rise in temperature. The average diameter increased from 80 nm to 170 nm. This implies that the growth rate along [0 0 2] direction is more sensitive to temperature compared to those along [0 0 1] and [1 0 1] directions. This statement was also supported by the fact that the ZnO nanorod arrays grown at lower temperature have more uniform size distribution. It is observed that the aspect ratio of the ZnO nanorods is increased with the increase of zinc acetate concentration because when the concentration is increased, the concentration of OH⁻ will also increase and then these OH⁻ ions can partially suppress the growth of as-deposited ZnO nano-crystallines along the c-axis direction [45]. Therefore, changing the growth temperature is another important means to control the morphology and aspect ratio of the ZnO nanorod arrays [18,19].

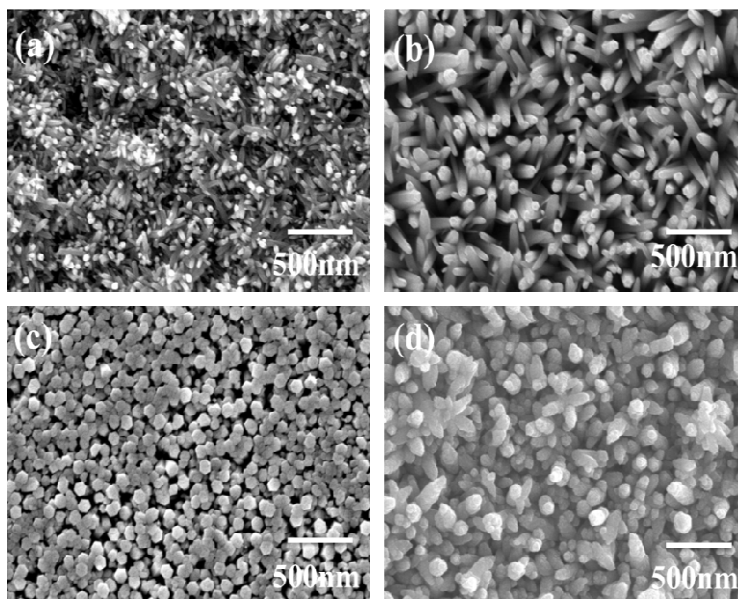


Fig 3: SEM micrograph of temperature dependent ZnO thin films deposited at (a) 65°C (b) 75°C (c) 85°C (d) 95°C.

The mechanism for the effect of precursor concentration and growth temperature can be elucidated with the chemical process of CBD and basic theory of crystal nucleation and growth. The chemical process involved in the growth of ZnO nanorods can be described as follows: $\text{Zn}(\text{CH}_3\text{COO})_2 \cdot 2\text{H}_2\text{O}$ provides Zn^{2+} ions required for building up ZnO nanorods, water molecules in the solution provide O^{2-} ions. Even though the exact function of ammonia solution during the growth is still unclear, it is believed to act as a weak base, which would slowly hydrolyze in the water solution and gradually produce OH⁻ [20]. The ZnO will form through dehydration of $\text{Zn}(\text{OH})_2$ and precipitate onto the substrates, leading to the formation of ZnO nanorods on the substrates.

Wurtzite ZnO has polar surface such as [0 0 2], and nonpolar surfaces such as [1 0 1] and [1 0 0]. The aspect ratio of the as grown ZnO nanorods will be determined by the relative growth rate of the polar surface and non-polar surface. With the increase of precursor concentration, the amount of $\text{Zn}(\text{OH})_2$ produced from precursor solution will increase correspondingly, which will increase the speed of growth during synthesis [21]. These processes are endothermic and will hinder ZnO nanorod arrays growth in the [0 0 2] directions, as a result, thicker nanorod arrays were obtained under higher precursor concentration. The temperature-dependent aspect ratio may also be understood considering the fact that the relative growth rate of the polar [0 0 2] surface and the non-polar [1 0 1] and [1 0 0] surfaces increase with the rise of growth temperature. Therefore, it is possible to control the morphology and aspect ratio of ZnO nanorod arrays on the substrate by adjusting the precursor concentration, growth temperature and time [22].

Optical properties of nanorods are important for many of their technological applications.

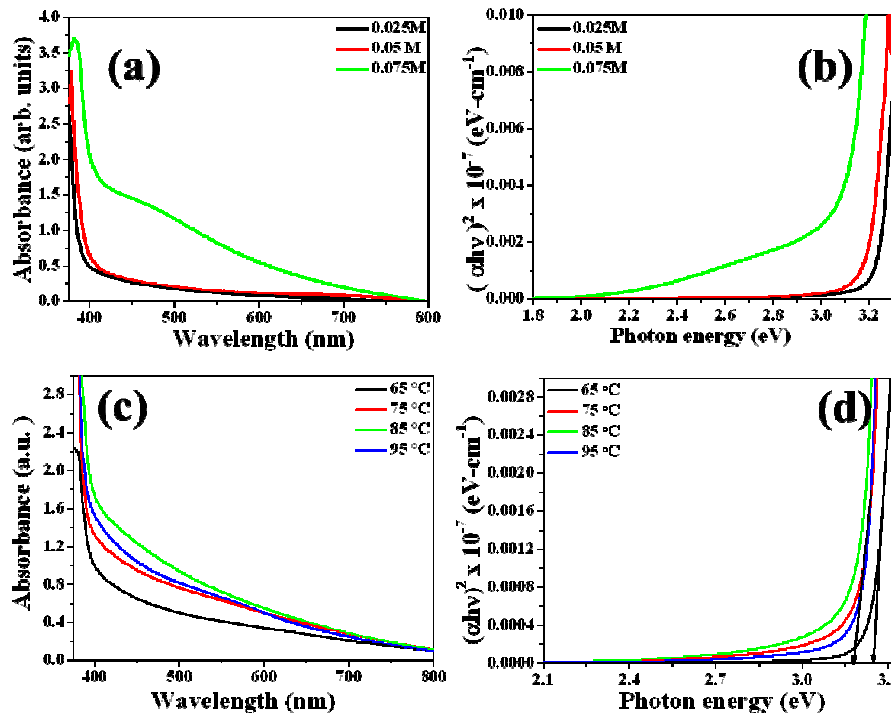


Fig 4 : Absorption spectra and Variation of $(\alpha h\nu)^2$ vs. $h\nu$ of the ZnO thin films (a) absorption spectra of precursor variation (b) band gap spectra of precursor variation (c) absorption spectra of temperature variation (d) band gap energy spectra of temperature variation.

The variation of absorbance (α) and band gap energy of ZnO film with the precursor concentration is shown in Fig. 4(a) (b). This spectrum reveals that low concentration ZnO film has low absorbance in the visible region, which is a characteristic of ZnO [23]. The absorbance has increased with increase in precursor concentration. The films shows absorption edge shift at low wavelength attributed to various factors such as electronic defects, vacancies [24] and nanorods imbedded in the amorphous phase [25]. Also Fig 4(c) shows with the variation in bath temperature from 65°C the absorbance increases till 85°C and further decreases for 95°C. All the films have sharp absorption edge at low wavelength. When a metal nanocluster was embedded in the dielectric matrices, an optical absorption spectrum was observed which accounts for the quantum size effect[26], or the limited metal free path of the conduction electrons [27] it is known that the system contains large no of hexagonal nanorods of ZnO. The role of the interaction between metal nanorods within the surface of substrate and temperature affect the linear optical absorption mechanism. Sharp ultraviolet absorption edges at approximately $\lambda=380\text{nm}$ are observed with the absorption edge being shifted to shorter wavelength at lower concentration. It can be clearly seen the shift in band edge in Fig. 4(b). The absorption coefficient α is calculated by applying the Tauc model [28]:

$$\alpha h\nu = A(h\nu - E_g)^m \quad (4)$$

Where, α is absorption coefficient, A is an energy-independent constant, m is a constant which determines type of the optical transition ($m= 1/2$ for allowed direct transitions and $m= 2$ for allowed indirect transitions) and E_g is the optical band gap. It is evaluated that the optical band gap of the ZnO film has a direct optical transition.

Fig.4 (b) shows plots of $(\alpha h\nu)^2$ Vs. $h\nu$ for the ZnO films deposited at different concentrations. As seen from these figures, the values of optical band gaps of the films decrease with increasing concentration. Namely, it shifts from 3.1025eV to 3.257eV as concentration varies from 0.025M to 0.075M. A blue shift in the absorption edge of ZnO film is also observed. This could mainly be attributed to the Burstein–Moss effect [29], since the absorption edge of a semiconductor shifts to shorter wavelengths with increase in carrier concentration. There are two main reasons of the shifting in the direct band gap with variation of concentration and temperature in the semiconductors [30]. The first reason is the effect of the lattice thermal expansion which is related to the change of electron energies with the volume. That is, the variation of E_g with temperature may be attributed to a shift in the relative positions of the valance and conduction bands due to the temperature dependence of the dilation of the lattice. The second reason is

the direct renormalization of the band energies due to the temperature dependence of the electron–phonon interactions. However, this shift accounts for only small fraction in the total variation of the gap energy.

CONCLUSION

ZnO nanorods arrays were successfully synthesized on the Si substrate by the wet chemical bath deposition (CBD) method. The effects of precursor concentration, growth temperature and time on nanorods morphology and aspect ratio were investigated systematically. The results indicate that it is possible to control the aspect ratio of ZnO nanorods on the substrate by adjusting the precursor concentration, growth temperature and time. It should be noted that only strong near-band edge UV emission peak were observed in room temperature PL spectra for the ZnO nanorods arrays on all substrates, yet the usually observed defect related deep level emissions were nearly undetectable, indicating high optical quality ZnO nanorod arrays could be achieved via this low temperature chemical approach. The high optical quality ZnO nanorod arrays presented here are very prospective for their applications in optoelectronic nanodevices, such as UV lasers, light-emitting diodes, and vertical field-effect transistor arrays.

REFERENCES

- [1] Martel R, Schmidt T, Shea H, Hertel T & Avouris P, *Appl Phys Lett*, 73 (1998) 2447.
- [2] Kim T, Choo D & Kang S, *Appl Phys Lett*, 80 (2002) 2168.
- [3] Singh I & Bedi R, *Appl Surf Sci*, 257 (2011) 7592.
- [4] Zhang W, Ganesh N, Mathias P.C & Cunningham B,
- [5] W. Zhang, N. Ganesh, P. C. Mathias, B. T. Cunningham, *Small* 4 (2008) 2199. Enhanced Fluorescence on a Photonic Crystal Surface Incorporating Nanorod Structures**
- [6] Schmidt-Mende L, MacManus-Driscoll J L, *Mater. Today* 10 (2007) 40.
- [7] Wang Z, *Mater Sci Eng R* 64 (2009) 33.
- [8] Robin I, Marotel P, Shaer A H EI, Petukhov V, Bakin A, Waag A, Lafossas M, Garcia J, Rosina M, Ribeaud A, Brochen S, Ferret P & Feuillet G, *J Cryst Growth* 311 (2009) 2172.
- [9] Yu D, Hu L, Li J, Hu H, Zhang H, Zhao Z & Fu Q, *Mater Lett* 62 (2008) 4063.
- [10] Guo Z, Zhao D X, Liu Y, Shen D, Zhang J & Liu B *Appl Phys Lett* 93 (2008) 1.
- [11] Guo H, Zhou J & Lin Z *Electrochem Commun* 10 (2008) 146.
- [12] Li Y, Yu L, Duan R, Shi P & Qin G *Solid State Commun* 129 (2004) 233.
- [13] Wu C L, Chang L, Chen H G, Lin C W, Chang T F, Chao Y C & Yan J K *Thin Solid Films* 498 (2006) 137.
- [14] Ahn C H, Han W S, Kong B H & Cho H K *Nanotechnology* 20 (2009) 015601.
- [15] Boyle D S, Govender K & Brien P O *Chem Commun* (2002) 80.
- [16] Xu S, Wei Y, Kirkham M & Wang Z L *J Am Chem Soc* J.
- [17] Liua X, Afzaal M, Badcock T, Dawson P & Brien P O *Mater Chem Phys* 127 (2011) 174.
- [18] Sun Y, Fox N A, Jason Riley D & Ashfold M N R, *J Phys Chem C* 112 (2008) 9234.
- [19] Goyal A & Kachhwaha S *Mater. Lett.* 68 (2012) 354.
- [20] Pawar B N, Cai G, Hama D, Mane R S, Ganesh T, Ghule A, Sharma R, Jadhav K D & Han S H *Sol Energy Mater Sol Cell* 93 (2009) 524.
- [21] Xu S, Lao C, Weintraub B & Wang Z L *J Mater Res* 23 (2008) 2072.
- [22] Zhang H, Yang D, Ji Y, Ma X, Xu J & Que D *J Phys Chem B* 108 (2004) 3955.
- [23] Chandramohan R, Vijayan T A, Arumugam S, Ramalingam H B, Dhanasekaran V, Sundaram K & Mahalingam T *Mater. Sci. Engg. B* 176 (2011) 152.
- [24] Pawar B N, Ham D H, Mane R S, Ganesh T, Cho B W & Han S H *Appl Surf Sci* 254 (2008) 6294.
- [25] Ghosh S & Mandal K, *J Mag Mag Mater* 322 (2010) 1979–1984.
- [26] Heng T S, Lau S P, Yu S F, Yang H Y, Wang L & Tanemura J S Chen, *Appl Phys Lett* 90 (2007) 032509-032512.
- [27] Prasada Rao T, Santhosh Kumar M C, Safarulla A, Ganesan V, Barman S R, Sanjeeviraja C, *Physica B* 405 (2010) 2226.
- [28] Cao L, Zhu L, Jang J, Zhao R, Ye Z & Zhao B 95 (2011) *Sol Energy Mater Sol Cells* 894.
- [29] Ma Q B, Ye Z Z, He H P, Zhu L P, Wang J R & Zhao B H *Mater Lett* 61 (2007) 2460.